

REACTION MECHANISMS IN $^{12}\text{C}+^{93}\text{Nb}$ SYSTEM: EXCITATION FUNCTIONS AND RECOIL RANGE DISTRIBUTIONS BELOW 7 MeV/u

TAUSEEF AHMAD^{*,¶}, I. A. RIZVI^{*}, AVINASH AGARWAL[†],
RAKESH KUMAR[‡], K. S. GOLDA[‡] and A. K. CHAUBEY[§]

^{*}Department of Physics, Aligarh Muslim University,
Aligarh-202002, India

[†]Department of Physics, Bareilly College, Bareilly-243005, India

[‡]Inter University Accelerator Centre, Aruna Asaf Ali Road,
P. O. Box 10502, New Delhi-110 067, India

[§]Department of Physics, Addis Ababa University,
P. O. Box 1176, Addis Ababa, Ethiopia

[¶]tau_ad@rediffmail.com

Accepted 14 July 2010

The experiments were performed to study excitation functions (EFs) of evaporation residues (ERs), i.e. $^{103,102,101}\text{Ag}$, $^{101,100,99}\text{Pd}$, $^{101,100}\text{Rh}$, ^{97}Ru , ^{96}Tc , ^{95}Tc , ^{94}Tc , $^{93}\text{Mo}^m$, $^{92}\text{Nb}^m$ populated in the reactions induced by ^{12}C on ^{93}Nb for exploring the reaction dynamics involved at energies $\approx 47\text{--}75$ MeV. The activation technique followed by offline γ -ray spectrometry has been employed to measure EFs. These measurements were simulated with other reported values available in literature as well as with theoretical predictions based on computer code PACE-2. The effect of variation of level density parameter involved in this code has also been studied. An excellent agreement was found between theoretical and experimental values in some of the fusion evaporation channels. However, significant enhancement of cross-section as observed in α -emission channels may be due to incomplete fusion (ICF) process and/or direct reaction process. To confirm the aforesaid reaction mechanism, Recoil Range Distributions (RRDs) of various ERs have been measured at ≈ 80 MeV. Moreover, an attempt is made to separate the percentage relative contributions of complete and incomplete fusion components from the analysis of the measured RRDs data. Further, the relative percentage ICF fraction, also estimated from EFs data, was found to be sensitive with the projectile energy.

Keywords: Excitation function; recoil range distribution; off-line gamma ray spectroscopy; complete fusion; incomplete fusion; heavy ion reactions.

PACS Number(s): 25.70 Gh, 25.70Jj

1. Introduction

A considerable interest to investigate reaction mechanism in heavy ion (HI) induced reactions at projectile energies in the range 4–10 MeV/u has become a recent phenomenon in the field of nuclear reactions.^{1–5} The study of HI interaction⁶ is quite

specific because of its complex structure and large momentum. The study of excitation function (EF) serves as a powerful tool to understand the reaction mechanism governing the collision dynamics, ranging from complete fusion (CF), incomplete fusion (ICF) to more complex pre-equilibrium (PE) process. Incomplete fusion has been studied by particle-gamma coincidence techniques⁷⁻⁹ mostly on heavy targets ($A \geq 120$). In a medium mass system, as undertaken in the present work, charge particle evaporation competes with neutron evaporation in the de-excitation process, leading to product formation via various different fusion modes and/or evaporation sequences making data interpretation more complex. Moreover, the presence of large numbers of evaporated charged particles may complicate the particle-gamma technique thus the mechanism of the incomplete fusion reactions is still not clearly understood. Several models¹⁰⁻¹³ have been proposed to explain the mechanism of ICF reactions but none succeeds in explaining all the features of ICF reactions at energies 4–7 MeV/u. Hence, the ICF reactions continue to be an active area of the investigation.

For a better understanding of complete, incomplete/PE emission and direct reaction dynamics, a wide range of experimental data is required. Although EFs for ^{93}Nb were measured by a few groups,^{14,15} their results differed from each other. Misaelides¹⁴ restricted himself to discussing the data concerning fusion reactions only not making any comment about ICF even for those reactions where α particles are emitted. Tomer *et al.*,¹⁵ however, discussed their results in the light of ICF, but they also not estimated ICF fraction and its sensitivity. Hence, the precise and accurate measurements are still needed. The present work, undertaken, attempts to measure the EFs for ^{93}Nb using $^{12}\text{C}^{6+}$ beam with the maximum number of possible γ -rays for a single reaction. Measurement of EFs is not the only criterion to determine the CF and/or ICF mechanism but that the RRDs have also been useful considerably. In order to separate the relative contributions of the CF and the ICF in $^{12}\text{C}+^{93}\text{Nb}$ system, hence the RRDs of several residues were measured and analyzed. Besides, an attempt has also been made to estimate ICF fraction from the measured EFs data. The present work not only supplements the data of the previous measurements^{14,15} but also provides a new cross-section database for various residues.

2. Experimental Details

The experiments were performed using 15 UD Pelletron facility at the Inter University Accelerator Centre (IUAC), New Delhi, India. Self-supporting ^{93}Nb targets of thickness $\approx 2.02 \text{ mg/cm}^2$ were prepared by rolling natural niobium of purity better than 99.9%. A stack of five targets of ^{93}Nb (each backed by Al degraders $\approx 2.08 \text{ mg/cm}^2$) was irradiated for ≈ 6.5 hours with a beam current $\approx 30 \text{ nA}$ at energy $\approx 75 \text{ MeV}$ in General Purpose Scattering Chamber (GPSC). For RRDs, thin target of ^{93}Nb of thickness ($\approx 100 \text{ }\mu\text{g/cm}^2$) was prepared by vacuum evaporation technique on to thin Al-foil of thickness $\approx 2.16 \text{ mg/cm}^2$. A stream of 13 Al

catcher foils (≈ 102 to $113 \mu\text{g}/\text{cm}^2$), prepared by the same technique, was used to stop the recoiling products. The thickness of each target was determined by the α -transmission method. The ^{12}C beam of energy ≈ 80 MeV was incident on front Al-surface for ≈ 4 hours with a beam fluence of $\approx 408.6 \mu\text{C}$. All the decay parameters of residues studied have been adopted from Table of Radioactive Isotopes.¹⁶ Post-irradiation analysis was performed using a high resolution, large volume (100 cc.) and pre-calibrated HPGe detector coupled with a data acquisition system. Various standard sources of known strength were used to determine the efficiency of the detector at various source-detector separations.¹⁷ The ERs were identified using the characteristic γ -rays as well as half-lives. Further, details of the experimental arrangement, formulation used and error analysis etc. are similar to the Ref. 3. The overall error in the present work is estimated to be $\leq 25\%$ including the statistical errors.

3. Results and Discussions

The experimentally measured cross-sections for the population of residues via CF and ICF processes are given in Tables 1 and 2 respectively. Here we have also tabulated the results of previous measurements by Misaelides¹⁴ and Tomer *et al.*¹⁵ Furthermore, we have compared the measured EFs with the calculated values obtained by using code PACE-2.¹⁸ This code uses the Monte Carlo procedure to determine the decay sequence of an excited nucleus. Details of this code are enumerated in Ref. 19. The effect of variation of level density parameter constant K ($= 8, 12$ and 16) of this code on calculated EFs is shown in Figs. 1–4. The measured EFs for residues populated via xn channels are shown in Figs. 1(a)–(c). Obviously these channels are populated only by CF. It may be ascertained from the figures that our measurements are consistent with PACE-2 ($K = 8$), thus firmly establishing a fine agreement between theoretical and experimental values. However, earlier measurements^{14,15} are lower than the theoretical values. In case of ^{93}Nb (C, p3n) ^{101}Pd reaction, the possibility of formation of ^{101}Pd may be via CF of ^{12}C with ^{93}Nb , and/or via the β^+ decay of its higher charge isobar precursor ^{101}Ag formed via reaction ^{93}Nb (C, 4n). Thus, the measured activity of ^{101}Pd may have contribution from both the independent production and from precursor decay. But our calculation¹⁹ shows that no precursor contribution has been found as shown in Fig. 2(a). Another feature of this plot is almost matching with the values in literature.^{14,15} Thus, our findings do not contradict with the conclusions drawn by Refs. 14, 15. As far as ^{93}Nb (C, p4n) ^{100}Pd and ^{93}Nb (C, p5n) ^{99}Pd reactions are concerned; our measurements here also are consistent with theoretical predictions. However, the values reported in Refs. 14, 15 are not in good agreement either with PACE-2 values or our measurements. From Figs. 1(a)–(c) and 2(a)–(c), it can be seen that xn ($x = 2, 3$ and 4) and pxn ($x = 3, 4$ and 5) products are populated solely via CF path. In ^{93}Nb (C, 2p2n) ^{101}Rh reaction, the ^{101}Rh is expected to be formed via CF of ^{12}C as well as ICF of ^8Be fragment. Our measured EFs for this

reaction (shown in Fig. 2(d)) indicate that this channel is populated via CF only. But the values reported by Misaelides¹⁴ are enhanced with respect to theoretical predictions which show some contribution from the ICF.

The EFs for the reaction $^{93}\text{Nb}(\text{C}, \alpha\text{n})^{100}\text{Rh}$ is shown in Fig. 3(a). An agreement between theoretical and experimental values exists below 65 MeV and above this energy significant enhancement of cross-section is found. This simply indicates that ^{100}Rh is populated via CF and ICF of ^8Be fragment both. Earlier measurements^{14,15} though fairly match with the present measurements and theoretical values but no such interpretations were provided by these authors.^{14,15} Regarding $^{93}\text{Nb}(\text{C}, \alpha\text{p}3\text{n})^{97}\text{Ru}$ reaction, it is inferred from Fig. 3(b) that our measured cross-sections are higher than the theoretical predictions as well as Ref. 14. This enhancement can be explained by the ICF of ^8Be fragment. However, Misaelides¹⁴ reports that residue ^{97}Ru is populated via CF only that could be one of the reasons for the difference in our and previous¹⁴ measurements.

As far as $(\text{C}, 2\alpha\text{xn})$ reaction channels are concerned, our measured cross-sections [shown in Figs. 3(c), (d) and 4(a)] are substantially higher than PACE-2 values and other values.^{14,15} This difference in cross-section simply indicates that these radionuclides, i.e. $^{96,95,94}\text{Tc}$ are populated via ICF. However, Tomer *et al.*¹⁵ show that ^{94}Tc data agree with the theoretical predictions indicating that ^{94}Tc being populated via CF only. Misaelides¹⁴ has termed the above mentioned channels as transfer reactions. The difference in data set (present and previous) can be explained by the fact that these channels may be populated via CF and/or ICF.

In case of $^{93}\text{Nb}(\text{C}, 2\alpha\text{p}3\text{n})^{93}\text{Mo}^{\text{m}}$ reaction [Fig. 4(b)], residue $^{93}\text{Mo}^{\text{m}}$ is expected to be populated via different routes mainly CF, ICF and direct reactions. Theoretical values remain negligible in this energy region, thus, not shown in Fig. 4(b). The data-set¹⁴ are not in agreement with our measurement and differ by an order of magnitude. This discrepancy between our measurement and Misaelides¹⁴ reported values may be due to the residue being populated in addition to direct reaction. Hence, this residue may be populated via ICF and direct reactions both. Finally, with reference to $^{93}\text{Nb}(\text{C}, ^{12}\text{C}, ^{13}\text{C})^{92}\text{Nb}^{\text{m}}$ reaction, $^{92}\text{Nb}^{\text{m}}$ may be populated via neutron pick up channel. The data trend of Misaelides¹⁴ and our measurements matches fairly but experimental values found to be substantially larger than those of PACE-2 [(as shown in Fig. 4(c)]. This difference in cross-section values may be attributed to direct reaction. Thus, the arguments presented by Misaelides¹⁴ for these residues $^{93}\text{Mo}^{\text{m}}$, $^{92}\text{Nb}^{\text{m}}$ are verified through our measurements.

The measured recoil ranges of ERs as a function of cumulative thickness of catcher foils are shown in Fig. 5. As shown in Figs. 5(a) and (b), the RRDs for $^{101,100}\text{Pd}$ isotopes produced via $(^{12}\text{C}, \text{p}3\text{n})$ and $(^{12}\text{C}, \text{p}4\text{n})$ channels respectively have a peak at only one value of cumulative catcher thickness ($\approx 770 \mu\text{g}/\text{cm}^2$). The RRDs of Pd isotopes are Gaussian having peaks at a thickness corresponding to the expected recoil range²⁰ of the composite nucleus ($^{105}\text{Ag}^*$) in Al. The single peak in above RRDs indicates that these products are formed via CF only.

Table 1. Experimentally measured cross-sections for ERs populated via CF.

Lab energy (MeV)	σ (^{103}Ag) (mb)	σ (^{102}Ag) (mb)	σ (^{101}Ag) (mb)	σ (^{101}Pd) (mb)	σ (^{100}Pd) (mb)	σ (^{99}Pd) (mb)	σ (^{101}Rh) (mb)
46.4* \pm 1.4	80.0* \pm 9.6	260.3* \pm 11.3		1.8 \pm 0.3			
48.4 ^b	18.8 ^b	158.6 ^b	5.9 ^b				
49.4 ^a	29.9 ^a	143.2 ^a		4.2 ^a			
54.0* \pm 1.4	38.2* \pm 3.9	615.4* \pm 125.3	60.3* \pm 6.6	57.8* \pm 11.8			2.8* \pm 0.4
56.3 ^b	8.8 ^b	152.1 ^b	61.1 ^b	102.8 ^b			
58.5 ^a	12.3 ^a	152.7 ^a	19.4 ^a	183.4 ^a			13.5 ^a
61.2* \pm 1.3	7.6* \pm 1.4	398.2* \pm 46.9	203.4* \pm 26.4	233.7* \pm 25.7	2.9* \pm 0.5	0.6 \pm 0.1	9.7* \pm 1.9
64.6 ^b		70.3 ^b	104. ^q ^b	523.0 ^b	46.4 ^b		
66.6 ^a	5.5 ^a	109.9 ^a	30.4 ^a	271.2 ^a	18.7 ^a		103.1 ^a
67.8* \pm 1.2		180.6* \pm 42.2	334.4* \pm 40.1	428.7* \pm 64.3	25.6* \pm 3.1	3.2* \pm 0.4	18.4* \pm 2.2
71.6 ^b		37.5 ^b	109.8 ^b		159.8 ^b	1.5 ^b	
72.7 ^a		46.9 ^a	29.1 ^a	372.1 ^a	80.0 ^a		67.4 ^a
73.9* \pm 1.1		40.1* \pm 10.3	305.3* \pm 30.5	339.9* \pm 33.7	113.3* \pm 15.9	6.1* \pm 0.9	22.8* \pm 2.5
77.4 ^a			18.4 ^a	291.6 ^a	166.8 ^a		103.1 ^a
78.3 ^b		8.0 ^b	35.5 ^b	400.1 ^b		6.5 ^b	

*Present measurements.

^aRef. 14.

^bRef. 15.

Table 2. Experimentally measured cross-sections for ERs populated via ICF.

Lab energy (MeV)	σ (^{100}Rh) (mb)	σ (^{97}Ru) (mb)	σ (^{96}Tc) (mb)	σ (^{95}Tc) (mb)	σ (^{94}Tc) (mb)	σ (^{93}Mo) (mb)	σ (^{92}Nb) (mb)
46.4* \pm 1.4	24.8* \pm 2.4				1.3* \pm 0.1		1.9* \pm 0.3
48.4 ^b	27.1 ^b		8.6 ^b	0.6 ^b			
49.4 ^a	31.4 ^a		5.8 ^a	0.9 ^a			1.1 ^a
54.0* \pm 1.4	15.2* \pm 0.9		13.2* \pm 3.8	119.4* \pm 9.9	15.1* \pm 2.0	1.4* \pm 0.1	3.9* \pm 0.4
55.9 ^b	14.4 ^b		24.6 ^b	2.7 ^b	0.3 ^b		
58.5 ^a	11.4 ^a		24.1 ^a	3.3 ^a			4.5 ^a
61.2* \pm 1.3	9.5* \pm 1.9		56.4* \pm 4.5	206.6* \pm 59.4	22.9* \pm 2.0	1.8* \pm 0.2	5.2* \pm 1.2
64.6 ^b	10.7 ^b		54.9 ^b	16.6 ^b	0.6 ^b		
66.6 ^a	10.8 ^a	1.0 ^a	32.0 ^a	8.9 ^a			6.4 ^a
67.8* \pm 1.2	25.1* \pm 3.6	17.8* \pm 3.9	101.2* \pm 10.7	386.3* \pm 52.3	45.9* \pm 5.0	3.6* \pm 0.5	14.9* \pm 1.3
71.6 ^b	30.2 ^b			48.5 ^b	2.2 ^b		
72.7 ^a	44.1 ^a	13.5 ^a	42.0 ^a	32.5 ^a	1.5 ^a	1.3 ^a	9.8 ^a
73.9* \pm 1.1	50.9* \pm 7.1	97.9* \pm 10.2	107.3* \pm 6.3	450.9* \pm 76.4	58.6* \pm 6.0	5.7* \pm 0.8	40.7* \pm 3.0
77.4 ^a	68.6 ^a	100.8 ^a	46.0 ^a	59.0 ^a	6.6 ^a	2.4 ^a	14.0 ^a
78.3 ^b	120.2 ^b		59.1 ^b	91.6 ^b			

*Present measurements.

^aRef. 14.^bRef. 15.

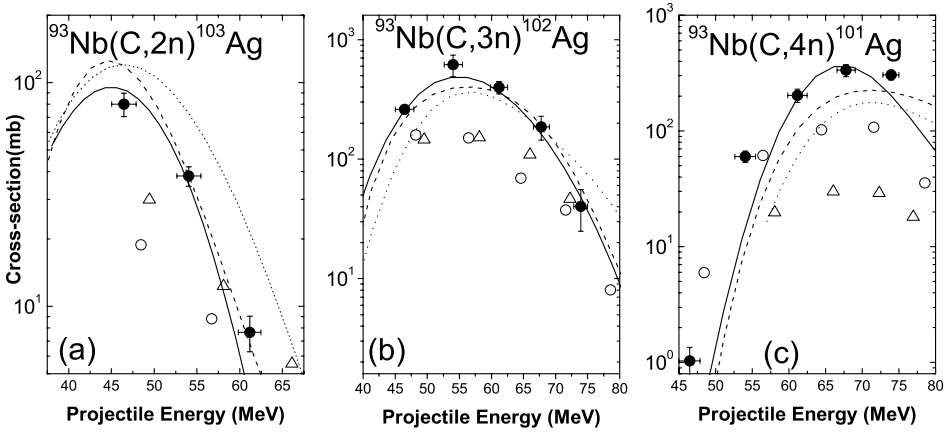


Fig. 1. Experimentally measured and theoretically calculated EFs using PACE-2. The dark circles indicate the experimental data points and the solid; dash and dot curves represent the polynomial fit to the PACE-2 predictions at different level density parameters (8, 12 and 16) respectively. Literature values^{14,15} are also shown by open upward triangle and open circle respectively.

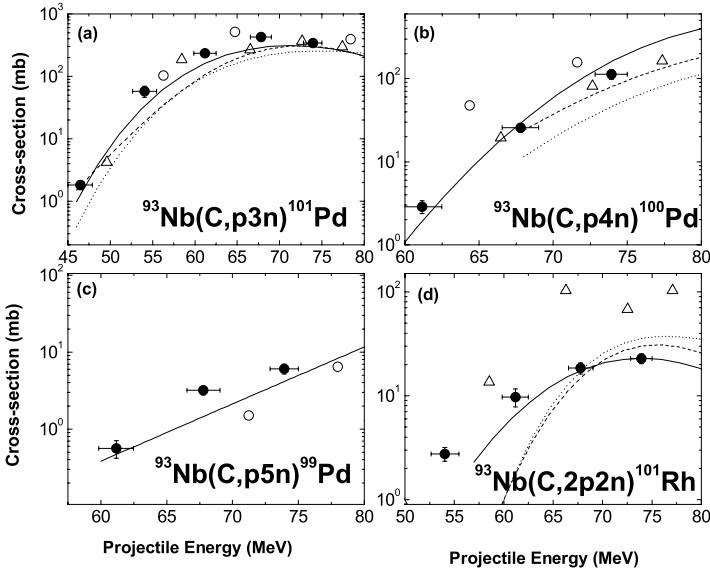


Fig. 2. Same as that of Fig. 1.

Regarding the $^{93}\text{Nb}(\text{C}, 2\alpha\text{n})^{96}\text{Tc}$ reaction, the RRDs show a dominant low range component due to the ICF of an α -particle (peak at $\approx 204 \mu\text{g}/\text{cm}^2$) while a long range tail as shown in Fig. 6(a) demonstrates almost a negligible CF part. In case of $^{93}\text{Nb}(\text{C}, 2\alpha 2\text{n})^{95}\text{Tc}$ and $^{93}\text{Nb}(\text{C}, 2\alpha 3\text{n})^{94}\text{Tc}$ reactions shown in Figs. 6(b) and 6(c), the RRDs have two peaks; one at relatively lower values of catcher

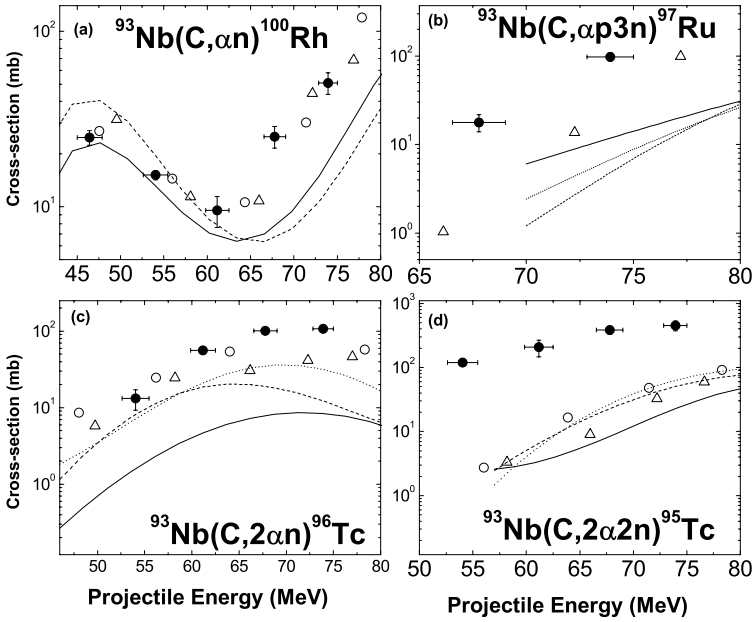


Fig. 3. Same as that of Fig. 1.

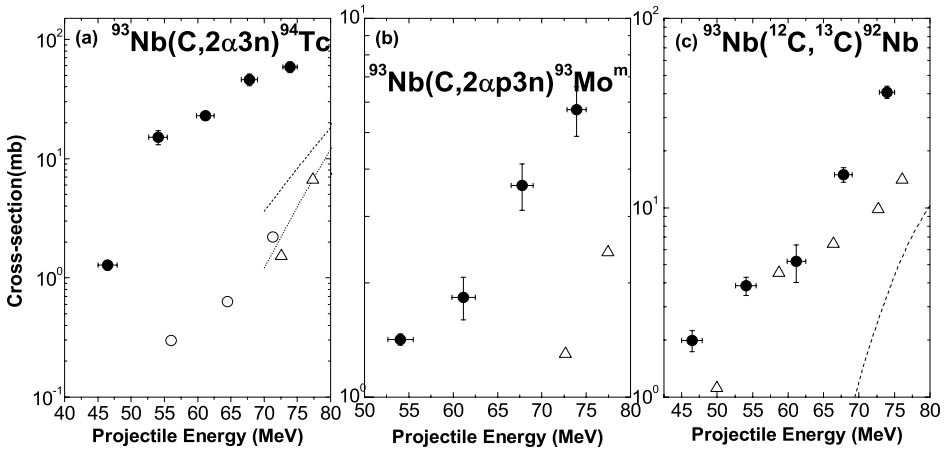


Fig. 4. Same as that of Fig. 1.

thickness $\approx 216/220 \mu\text{g}/\text{cm}^2$ (due to α fusion) and the other at $\approx 702/750 \mu\text{g}/\text{cm}^2$ (due to ^{12}C fusion). The relative contribution of the ICF of α -particle in the population of ^{95}Tc and ^{94}Tc residues is found to be $\approx 49.1\%$ and 40.3% respectively [Figs. 6(b) and (c)]. In the light of the above facts, it may be concluded that the ICF plays an important role in the heavy-ion reactions.

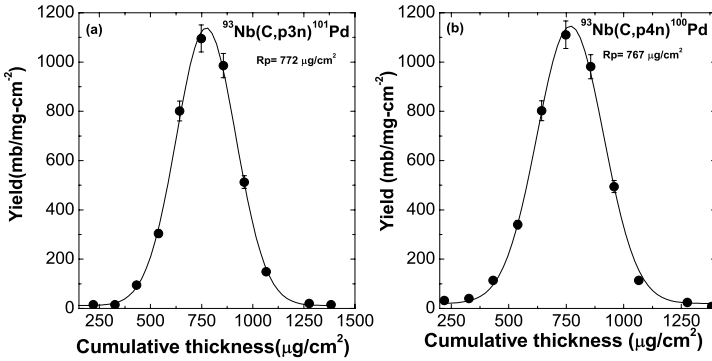


Fig. 5. Gaussian fit to the experimentally measured RRDs for CF channels.

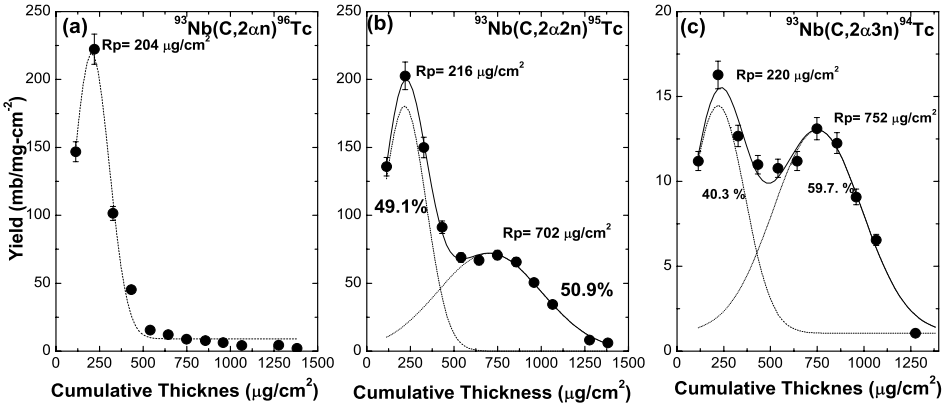


Fig. 6. Gaussian fit to the experimentally measured RRDs for ICF channels.

Though, it is not a usual practice to obtain directly relative ICF contribution from the EFs measurement, an attempt has been made here to find the ICF contribution. The difference in the experimentally measured cross-section values and the PACE-2 predictions indicates the ICF contribution. For $^{12}\text{C} + ^{93}\text{Nb}$ system, the contribution coming from all ICF channels ($\sum \sigma_{\text{ICF}}$) and the sum of all CF channels ($\sum \sigma_{\text{CF}}$) obtained from PACE-2 calculations are plotted along with the total fusion cross-section in Fig. 7(a). It can be observed from the above figure that the CF component has measurable contribution even at ≈ 47 MeV, while ICF contribution seems to start from ≈ 54 MeV. Further, the separation between the plots for $\sum \sigma_{\text{TF}}$ (solid circle) and $\sum \sigma_{\text{CF}}$ (solid triangle) increases with projectile energy (Fig. 7(a)) which indicates that the ICF contributes larger production yield at relatively high projectile energies. This may be due to the fact that probability of the break-up of the incident ion ^{12}C into alpha cluster ($^8\text{Be} + \alpha$) increases as the projectile energy increases. In addition to it, the data appears to support the sensitivity of ICF as

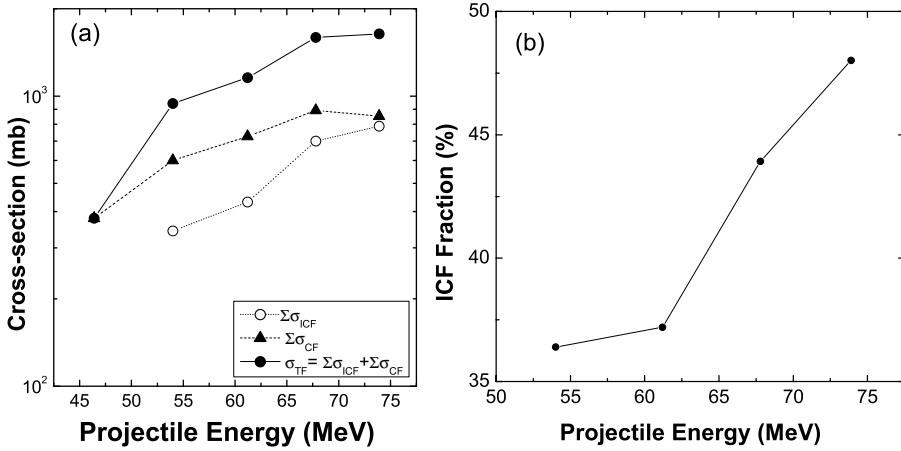


Fig. 7. (a, b) Total fusion probability along with ICF fraction (%) as a function of projectile energy.

projectile energy, as inferred by Morgenstern *et al.*²¹ To investigate the effect of above variable on the relative contributions of CF and ICF, the percentage ICF fraction (F_{ICF}) for $^{12}\text{C}+^{93}\text{Nb}$ system has been estimated from the experimentally measured cross-section.²² The ICF fraction has been deduced at different energies and is plotted as a function of projectile energy [Fig. 7(b)]. It can be observed from the figure that at the threshold of ICF (i.e. ≈ 54 MeV), the relative percentage ICF fraction is found to be 36.4%, and it increases with the increasing projectile energies. At the maximum studied energy (i.e. ≈ 75 MeV) the F_{ICF} approaches to 48.0% of total fusion cross-section.

4. Conclusions

In the present work, EFs for fourteen reactions populated in the $^{12}\text{C}+^{93}\text{Nb}$ system in the energy range ≈ 47 –75 MeV have been measured and compared with predictions of code PACE-2. The above measurements found consistent with the theoretical predictions based on the model code PACE-2. It has also been observed that, in general, residues are not only populated via CF but ICF is also found to play an important role. Moreover, the direct reactions are also found to be significant in the population of radio-nuclides $^{93}\text{Mo}^m$ and $^{92}\text{Nb}^m$. To find out the component of CF and ICF in a particular reaction channel, RRDs have been studied. From the RRDs analysis it may be stated that ICF is also a process of greater importance at these energies and hence while predicting the total reaction cross-section, the contribution coming from the ICF must be taken into consideration. Further, the ICF fraction from the EFs data has been estimated and found to be dependent on the incident projectile energy. Moreover, for a perfect modeling of the ICF process, it is quite desirable to perform more detailed experiments consisting of the measurement of spin distribution of residues populated by CF as well as

ICF, using particle-gamma coincidence technique both at relatively low and higher bombarding energies.

Acknowledgments

The authors are thankful to the Director, IUAC, New Delhi, India for extending all the facilities for carrying out the experiment. We also thank the Chairman, Department of Physics, AMU, Aligarh, India for providing all the necessary facilities. The financial assistance to one of the authors (AA) from DST, New Delhi, India in the form of Fast Track Young Scientist Scheme vide project Ref. SR/FTP/PS-08-2006 is highly acknowledged. We are obliged to Er. Abilash, IUAC, New Delhi for providing technical help in the preparation of targets required for the experiment.

References

1. D. P. Singh *et al.*, *Phys. Rev. C* **80** (2009) 014601.
2. D. Singh *et al.*, *Phys. Rev. C* **79** (2009) 054601.
3. A. Agarwal *et al.*, *Int. J. Mod. Phys. E* **17** (2008) 393.
4. T. Ahmad *et al.*, *Nucl. Phys. Sym.* **52** (2007) 313.
5. S. Mukherjee *et al.*, *Int. J. Mod. Phys. E* **15** (2006) 237.
6. P. E. Hodgson, *Nuclear Heavy Ion Reactions* (Clarendon, Oxford, 1978).
7. T. Inamura *et al.*, *Phys. Lett. B* **68** (1977) 51.
8. K. Siwek-Wilezyska *et al.*, *Nucl. Phys. A* **330** (1979) 150.
9. H. Yamada *et al.*, *Phys. Rev. C* **24** (1981) 2565.
10. T. Udagawa and T. Tamura, *Phys. Rev. Lett.* **45** (1980) 1311.
11. J. Wilczyński *et al.*, *Nucl. Phys. A* **373** (1982) 109.
12. J. P. Bendorf *et al.*, *Nucl. Phys. A* **333** (1980) 285.
13. M. Blann, *Phys. Rev. C* **31** (1985) 1285.
14. P. Misaelides, *Radiochim. Acta* **28** (1981) 1.
15. B. S. Tomer *et al.*, *Z. Phys. A* **343** (1992) 223.
16. E. Browne and R. B. Firestone, *Table of Radioactive Isotopes* (John Wiley & Sons, New York, 1986).
17. A. Agarwal *et al.*, *Can. J. Phys.* **86** (2008) 495.
18. A. Gavron, *Phys. Rev. C* **21** (1980) 230.
19. T. Ahmad, Ph.D. Thesis, Aligarh Muslim University, 2008.
20. L. C. Northcliffe and R. F. Schilling, *Atom. Data Nucl. Data Tables A* **7** (1970) 264.
21. H. Morgenstern *et al.*, *Phys. Rev. Lett.* **52** (1984) 1104.
22. P. P. Singh *et al.*, *Phys. Rev. C* **77** (2008) 014607.